23. Passey, Q. R. & Melosh, H. J. Effects of atmospheric breakup on crater field formation. *Icarus* **42,** 211–233 (1980).
24. Melosh, H. J. *Impact Cratering: A Geological Process* (Oxford Univ. Press, Oxford, 1989).
25. Schmidt, R. M. & Housen, K. R. Some recent advances in the scaling of impact and explosion cratering. *Int. J. Impact Eng.* **5,** 543–560 (1987).
26. Ivanov, B. A., *et al.* in *Chronology and Evolution of Mars* (ed. Kallenbach, R.) 87–104 (Kluwer, Dordrecht, 2001).
27. Hartmann, W. K. Martian cratering VI: Crater count isochrons and evidence for recent volcanism from Mars Global Surveyor. *Meteorit. Planet. Sci.* **34,** 167–177 (1999).
28. Bland, P. A. *et al.* The flux of meteorites to the Earth over the last 50,000 years. *Mon. Not. R. Astron. Soc.* **283,** 551–565 (1996).

Acknowledgements We thank B. Ivanov, W. Hartmann and P. Brown for providing cratering data, flux data, and for discussions, and B. Ivanov, H. J. Melosh, V. Shuvalov, J. Morgan, E. Pierazzo and M. Gounelle for suggestions that improved earlier drafts of this manuscript. This work benefited greatly from comments and suggestions from C. Chapman. N.A. thanks RFBR for support, and P.A.B. thanks the Royal Society for support.

Competing interests statement The authors declare that they have no competing financial interests.

Correspondence and requests for materials should be addressed to P.A.B. (p.a.bland@imperial.ac.uk).

Nanometre-scale displacement sensing using a single electron transistor

Robert G. Knobel*† **& Andrew N. Cleland***

* *Department of Physics and iQUEST, University of California, Santa Barbara, California 93106, USA*

It has been a long-standing goal to detect the effects of quantum mechanics on a macroscopic mechanical oscillator[1–3]. Position measurements of an oscillator are ultimately limited by quantum mechanics, where 'zero-point motion' fluctuations in the quantum ground state combine with the uncertainty relation to yield a lower limit on the measured average displacement. Development of a position transducer, integrated with a mechanical resonator, that can approach this limit could have important applications in the detection of very weak forces, for example in magnetic resonance force microscopy[4] and a variety of other precision experiments[5–7]. One implementation that might allow near quantum-limited sensitivity is to use a single electron transistor (SET) as a displacement sensor[8–11]: the exquisite charge sensitivity of the SET at cryogenic temperatures is exploited to measure motion by capacitively coupling it to the mechanical resonator. Here we present the experimental realization of such a device, yielding an unequalled displacement sensitivity of 2×10^{-15} m Hz$^{-1/2}$ for a 116-MHz mechanical oscillator at a temperature of 30 mK—a sensitivity roughly a factor of 100 larger than the quantum limit for this oscillator.

A classical simple harmonic oscillator, in equilibrium with its environment at temperature T, will have an average total energy $k_B T$. The position of the oscillator fluctuates continuously, with a root mean square displacement amplitude $\delta x = (k_B T/m\omega_0^2)^{1/2}$ for an oscillator of mass m and resonant frequency $f_0 = \omega_0/2\pi$. This classical displacement amplitude can be made arbitrarily small by reducing the temperature. One implication of quantum mechanics, however, is that the quantized nature of the oscillator energy yields an intrinsic fluctuation amplitude, the 'zero-point motion' $\delta x_{zp} = (\hbar/2m\omega_0)^{1/2}$. This is achieved for temperatures T well below the energy quantum, $T \ll T_Q \equiv \hbar\omega_0/k_B$. A second implication of quantum mechanics is that the instrument used to measure the position of the oscillator will necessarily perturb it, further limiting the possible measurement resolution, as quantified by the Heisenberg uncertainty principle. A continuous measurement of the average position of an oscillator, using a quantum-limited amplifier, is thus limited to $\sqrt{2}$ times the zero-point motion, or $\delta x_{meas} \geq (\hbar/m\omega_0)^{1/2}$. We note that 'back-action evading' techniques have in principle unlimited measurement precision, although these yield less information and are still subject to zero-point fluctuations if the measurement is slower than the oscillator relaxation time[1,12].

A 1-GHz nanomechanical flexural resonator was recently demonstrated[13]. This resonator would have $T_Q = 50$ mK, so when operated on a dilution refrigerator at 10 mK, the inequality $T \ll T_Q$ could be reached. A resonator with similar dimensions would be a candidate for detecting the transition from classical to quantum noise, because the small mass gives a relatively large zero-point displacement noise, $\delta x_{zp} \approx 2 \times 10^{-14}$ m. In terms of the spectral displacement noise density, this corresponds to $S_x^{1/2} = 5 \times 10^{-18}$ m Hz$^{-1/2}$ on resonance, fairly small due to the relatively low quality factor $Q \approx 500$. Techniques to measure the displacement of large-scale resonators, such as optical interferometry or electrical parametric transducers[1,14,15], can achieve better displacement noise limits than this, but the larger mass of the resonator makes reaching the quantum limit more difficult. Such techniques do not scale well to nanomechanical resonators, and other techniques more applicable to these size scales[16,17] are unlikely to approach quantum-limited sensitivity. The single electron transistor provides a possible system in which sufficient sensitivity can be achieved.

The single-electron transistor (SET) consists of a conducting island separated from leads by low-capacitance, high-resistance tunnel junctions. The current through the SET is modulated by the charge induced on its gate electrode, with a period e, the charge of one electron. The SET is the most sensitive electrometer[18,19], with a demonstrated sensitivity below $10^{-5}\ e\,\mathrm{Hz}^{-1/2}$. The motion of a nanomechanical resonator may be detected by capacitively coupling the gate of the SET to a metal electrode placed on the resonator, and biasing the electrode at a constant voltage V_{beam} (see Fig. 1). The capacitance C between the SET and the beam then has a coupled charge $q = V_{beam}C$. As the beam vibrates in the x direction, in the

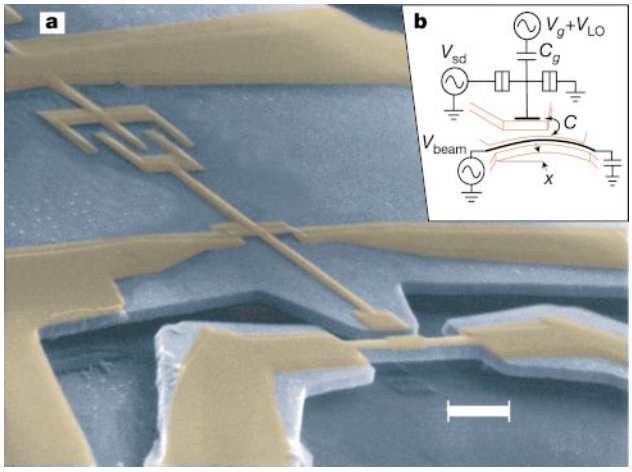

Figure 1 The device used in the experiment. **a**, Scanning electron micrograph of the device, showing the doubly clamped GaAs beam, and the aluminum electrodes (coloured) forming the single electron transistor and beam electrode. Scale bar, 1 μm. The Al/AlO_x/Al tunnel junctions have approximately 50×50 nm^2 overlap. **b**, A schematic of the mechanical and electrical operation of the device.

† Present address: Department of Physics, Queen's University, Kingston, Ontario K7L 3N6, Canada.

plane of the device, the resulting variation in capacitance ΔC will modulate the charge induced on the SET, $\Delta q = V_{\rm beam}\Delta C$, changing the SET source–drain current. As the voltage $V_{\rm beam}$ is increased, the charge modulation Δq and the sensitivity to the resonator motion will increase. However, the source-drain current is due to the stochastic flow of electrons through the SET, so the centre island's voltage fluctuates randomly. This causes a fluctuating 'back-action' force on the beam. This force increases as $V_{\rm beam}$ increases, resulting in a voltage for which the total noise is minimized. The displacement sensitivity at this optimal voltage is calculated[9,10] to be of order $10^{-16}\,{\rm m\,Hz^{-1/2}}$, approaching the sensitivity needed to measure quantum effects.

Our device (Fig. 1) consists of a 3 μm long × 250 nm wide × 200 nm thick doubly-clamped beam of single-crystal GaAs, capacitively coupled to an aluminum SET, located 250 nm from the beam. The beam was patterned using electron beam lithography and etched from a GaAs heterostructure using a sequence of reactive ion etching and dilute HF wet etching[20]. The SET was formed through double-angle shadow evaporation, using a pattern defined in a second step of electron-beam lithography[21,22]. The device was mounted on a dilution refrigerator and cooled to 30 mK. All electrical leads were filtered[23]. An out-of-plane 8 T magnetic field was applied to drive the aluminum out of the superconducting state, and to provide a field for actuation and sensing of the beam motion.

The beam was driven using the magnetomotive technique, in which an alternating current I through the beam electrode, along its length ℓ in the presence of the magnetic field B, generates a Lorentz force $F = I\ell B$. We measured the induced electromotive force (EMF) $\mathscr{E}$ developed along the beam owing to its resulting motion through the magnetic field[16,24,25] by measuring the reflected and transmitted power. The beam vibrates in its fundamental in-plane mode with a resonant frequency $f_0 = 116.7$ MHz (see Fig. 2). The measured EMF fits well to a lorentzian function with a quality factor $Q \approx 1700$. The beam displacement Δx is related to the EMF $\mathscr{E}$ by[25]:

$$\Delta x = \frac{\mathscr{E}}{\xi \ell B \omega} \qquad (1)$$

where $\xi = 0.523$ is an integration constant. We thus determine the displacement Δx as a function of power P, as shown in Fig. 2, yielding the resonator mass $m = 2.84 \times 10^{-15}$ kg and effective spring constant $k = 1{,}530\,{\rm N\,m^{-1}}$.

The SET was characterized using low-frequency electrical measurements, giving a series junction resistance $R_{J1} + R_{J2} = 200\,{\rm k\Omega}$, a gate capacitance $C_g = 0.59$ fF, a coupling capacitance between the beam electrode and the SET of $C = 0.13$ fF, and a total SET island capacitance $C_\Sigma = 1.3$ fF. In order to detect motion at the resonant frequency of the beam, the SET was operated as a mixer[11], with a local oscillator (LO) voltage $V_{\rm LO}$ applied to the gate at a frequency offset from the drive frequency by an intermediate frequency (IF) of less than 1 kHz ($f_{\rm IF} = |f_{\rm LO} - f|$). The SET was biased so as to give optimum mixing signal, with $V_{\rm sd} \approx e/C_\Sigma$ and the dc gate voltage adjusted to give peak dc current. The $V_{\rm LO}$ amplitude was set to give maximum signal gain, with coupled charge at the LO frequency $q_{\rm LO} \approx 0.4e$. The voltage across the SET was measured at the intermediate frequency.

Figure 3a shows the mixer signal for a drive power $P = -125$ dBm. Using the magnetomotive calibration, this corresponds to an extrapolated amplitude of $\Delta x = 2.3 \times 10^{-14}$ m on resonance. The charge Δq detected by the SET is due to the change in coupling capacitance times the beam voltage, $\Delta q = V_{\rm beam}\Delta C$, as well as secondary signals due to the induced EMF, and capacitively coupled charge due to cable resonances and ohmic losses. The former is very small compared to the direct signal (less than 1%), and the second varies slowly with frequency. Thus the total signal detected by the SET has the form of a lorentzian, plus a background with an arbitrary phase, as shown in Fig. 3a.

The quality factor Q and resonant frequency f_0 obtained using the SET were the same as those from the magnetomotive technique, and the amplitude varied as $P^{1/2}$. The SET response is found to be 9.9

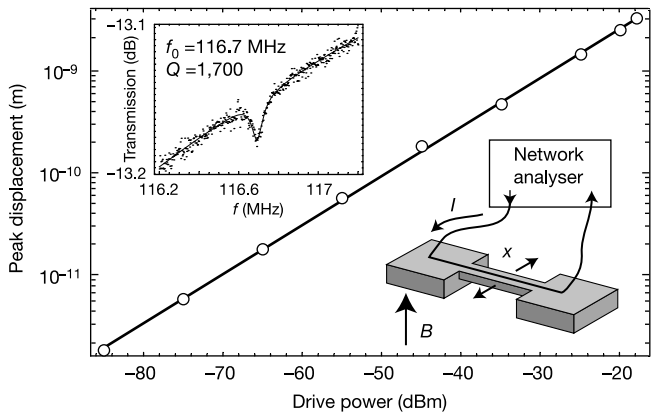

Figure 2 Magnetomotive measurements of the beam resonance. Upper inset, Raw magnetomotive transmission data (20 averages, 10 Hz bandwidth) as a function of drive frequency f, for a drive power $P = -85$ dBm, with a fit of a lorentzian line shape with a linear background. The fit yields the resonance frequency $f_0 = 116.7$ MHz and quality factor $Q = 1700$. The main plot shows the measured midpoint displacement Δx of the beam driven at its frequency resonance $f = f_0$, as a function of magnetomotive drive power P at 30 mK and in an 8 T magnetic field. The fit response $\Delta x = 839\sqrt{P}$ nm/W$^{1/2}$ (solid line), with the beam's known physical geometry (lower inset), corresponds to an effective spring constant $k = 1{,}530\,{\rm N\,m^{-1}}$ and resonator mass $m = 2.84 \times 10^{-15}$ kg.

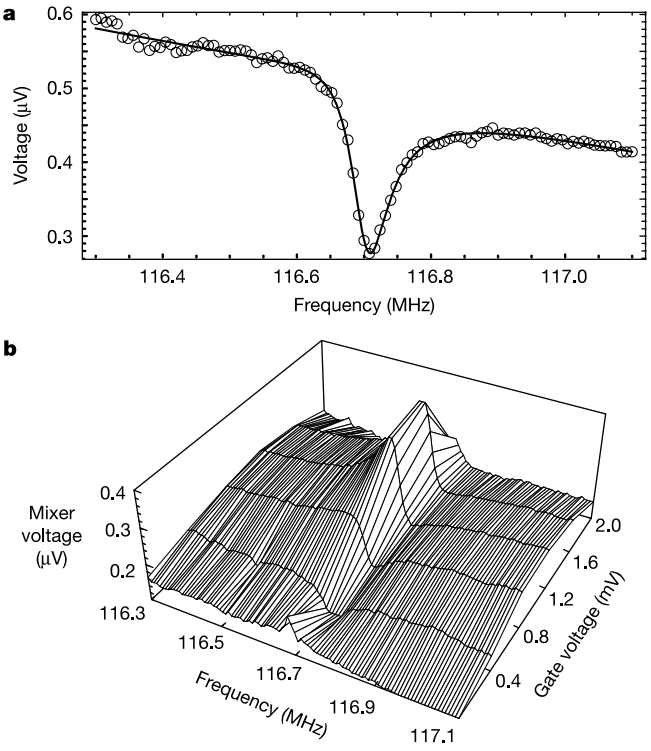

Figure 3 Single electron transistor measurement of the beam motion. **a**, Intermediate frequency voltage (SET mixer output) as a function of beam drive frequency, for $P = -125$ dBm drive power. The solid line is a fit to a lorentzian plus linear background with arbitrary phase. The beam electrode had a d.c. voltage $V_{\rm beam} = 5$ V, the LO power was −70 dBm, and the IF was 151 Hz. The SET gate voltage was tuned to give maximum signal. **b**, IF voltage for $P = -115$ dBm drive power, as a function of d.c. gate voltage and drive frequency. The slowly varying background interferes with the resonance signal, whose phase varies with the gate voltage.

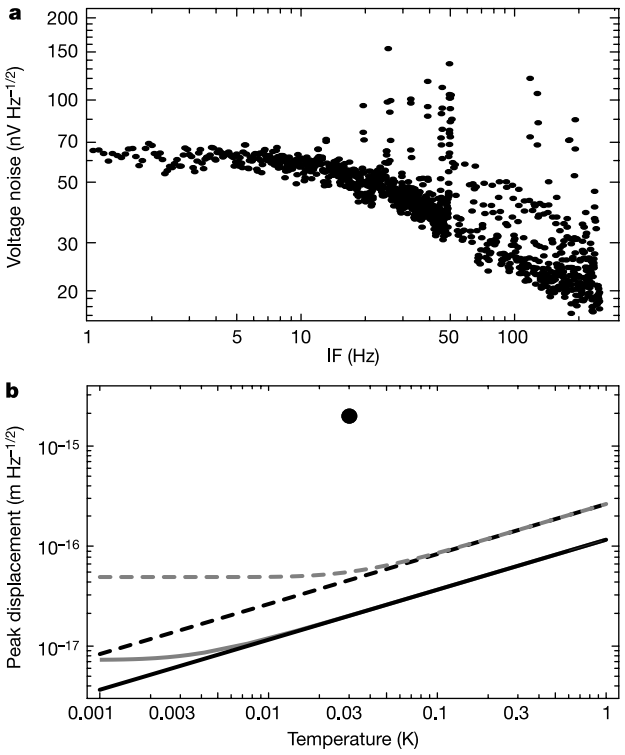

Figure 4 Noise and quantum limits for the device. **a**, Output voltage noise $S_V^{1/2}$ as a function of mixer intermediate frequency in the same configuration as used for the driven beam measurements (LO = −70 dBm, $f_{LO} = 100$ MHz, $V_{sd} \approx e/C_\Sigma$, $V_{beam} = 5$ V, $B = 8$ T, $T = 30$ mK). For the displacement measurements, an intermediate frequency of 151 Hz was used, corresponding to a noise level of about 20 nV Hz$^{-1/2}$. **b**, Calculated displacement noise for two resonators, the resonator measured in this experiment (solid lines) and for a hypothetical 1–GHz resonator (dashed lines), fabricated from GaAs with dimensions 450 × 50 × 40 nm and $Q = 10^4$. The black lines correspond to the thermal noise and the grey lines include the back-action noise and zero-point motion in an ideal quantum-limited position measurement. The measured noise of our device is indicated by the black circle.

Δx Vμm^{-1}, proportional to the displacement Δx, when the SET is biased optimally, with a LO frequency offset from the beam drive signal by 151 Hz. As the SET gate voltage is varied from the optimum value, Fig. 3b, the sensitivity decreases and interference with the background becomes more pronounced. The resonant signal decreases linearly with magnetic field B, and increases linearly with V_{beam}.

Figure 4a shows the output voltage noise of the SET mixer. For the intermediate frequency used (151 Hz), the noise (~20 nV Hz$^{-1/2}$) is dominated by the second-stage amplifier. The displacement sensitivity can be calculated from the SET response: We find a peak sensitivity of $S_x^{1/2} \approx 2.0 \times 10^{-15}$ m Hz$^{-1/2}$.

We can now evaluate the potential for quantum-limited detection: In Fig. 4b we show the calculated thermal and quantum noise for this beam, and for a 1–GHz resonator, which would be in its quantum ground state at the base temperature of our dilution refrigerator. We see that the detector noise is ~100 times larger than the thermal noise of the measured beam, and about a factor of ~20 larger than the quantum noise of a 1–GHz resonator with $Q = 10^4$. By using improved electronics and impedance matching, the second-stage noise could be reduced by roughly a factor of ten, and better lithography could reduce the SET-beam separation, increasing the SET response. A higher quality factor would yield larger signals in both the thermal and quantum limits; experimentally the Q is observed to reduce as the resonators are made smaller, at least partly due to surface damage and contamination. Flash heating of resonators in vacuum has been demonstrated to yield significantly higher quality factors[26,27], a technique which could be applied here. The expected increase in displacement sensitivity using a combination of these techniques could, in a second–generation device, allow measurement in the quantum-limited regime.

In conclusion, we have demonstrated an ultrasensitive, potentially quantum-limited displacement sensor based on a single-electron transistor, enabling us to read out the motion of a nanomechanical resonant beam at its resonant frequency. The device has a displacement sensitivity of 2.0×10^{-15} m Hz$^{-1/2}$ at the 116.7–MHz resonant frequency of the mechanical beam, limited by the noise in the conventional electronics. □

Received 28 March; accepted 29 May 2003; doi:10.1038/nature01773.

1. Bocko, M. F. & Onofrio, R. On the measurement of a weak classical force coupled to a harmonic oscillator: Experimental progress. *Rev. Mod. Phys.* **68,** 755–790 (1996).
2. Braginsky, V. B. & Khalili, F. Y. *Quantum Measurement* (Cambridge Univ. Press, Cambridge, 1992).
3. Cho, A. Researchers race to put the quantum in mechanics. *Science* **299,** 36–37 (2002).
4. Sidles, J. A. *et al.* Magnetic resonance force microscopy. *Rev. Mod. Phys.* **67,** 249–265 (1995).
5. Armour, A. D., Blencowe, M. P. & Schwab, K. C. Entanglement and decoherence of a micromechanical resonator via coupling to a cooper-pair box. *Phys. Rev. Lett.* **88,** 148301 (2002).
6. Tobar, M. E. & Blair, D. G. Sensitivity analysis of a resonant-mass gravitational wave antenna with a parametric transducer. *Rev. Sci. Instrum.* **66,** 2751–2759 (1995).
7. Long, J. C. *et al.* Upper limits to submillimetre-range forces from extra space-time dimensions. *Nature* **421,** 922–925 (2003).
8. White, J. D. An ultra high resolution displacement transducer using the Coulomb blockade electrometer. *Jap. J. Appl. Phys 2* **32,** L1571–L1573 (1993).
9. Blencowe, M. P. & Wybourne, M. N. Sensitivity of a micromechanical displacement detector based on the radio-frequency single-electron transistor. *Appl. Phys. Lett.* **77,** 3845–3847 (2000).
10. Zhang, Y. & Blencowe, M. P. Intrinsic noise of a micro-mechanical displacement detector based on the radio-frequency single-electron transistor. *J. Appl. Phys.* **91,** 4249–4255 (2002).
11. Knobel, R. & Cleland, A. N. Piezoelectric displacement sensing with a single-electron transistor. *Appl. Phys. Lett.* **81,** 2258–2260 (2002).
12. Caves, C. M., Thorne, K. S., Drever, R. W. P., Sandberg, V. D. & Zimmermann, M. On the measurement of a weak classical force coupled to a quantum-mechanical oscillator. 1. Issues of principle. *Rev. Mod. Phys.* **52,** 341–392 (1980).
13. Huang, X. M. H., Zorman, C. A., Mehregany, M. & Roukes, M. L. Nanoelectromechanical systems: Nanodevice motion at microwave frequencies. *Nature* **421,** 496 (2003).
14. Abramovici, A. *et al.* Improved sensitivity in a gravitational wave interferometer and implications for LIGO. *Phys. Lett. A* **218,** 157–163 (1996).
15. Mamin, H. & Rugar, D. Sub-attonewton force detection at millikelvin temperature. *Appl. Phys. Lett.* **79,** 3358–3360 (2001).
16. Cleland, A. N. & Roukes, M. L. External control of dissipation in a nanometer-scale radiofrequency mechanical resonator. *Sensors Actuators A* **72,** 256–261 (1999).
17. Beck, R. G. *et al.* GaAs/AlGaAs self-sensing cantilevers for low temperature scanning probe microscopy. *Appl. Phys. Lett.* **73,** 1149–1151 (1998).
18. Schoelkopf, R. J., Wahlgren, P., Kozhevnikov, A. A., Delsing, P. & Prober, D. E. The radiofrequency single-electron transistor (rf-SET): A fast and ultrasensitive electrometer. *Science* **280,** 1238–1242 (1998).
19. Devoret, M. H. & Schoelkopf, R. J. Amplifying quantum signals with the single-electron transistor. *Nature* **406,** 1039–1046 (2000).
20. Cleland, A. N., Aldridge, J. S., Driscoll, D. C. & Gossard, A. C. Nanomechanical displacement sensing using a quantum point contact. *Appl. Phys. Lett.* **81,** 1699–1701 (2002).
21. Fulton, T. A. & Dolan, G. J. Observations of single-electron charging effects in small tunnel junctions. *Phys. Rev. Lett.* **59,** 109–112 (1987).
22. Knobel, R., Yung, C. S. & Cleland, A. N. Single-electron transistor as a radio-frequency mixer. *Appl. Phys. Lett.* **81,** 532–534 (2002).
23. Martinis, J. M., Devoret, M. H. & Clarke, J. Experimental tests for the quantum behavior of a macroscopic degree of freedom: The phase difference across a Josephson junction. *Phys. Rev. B* **35,** 4682 (1987).
24. Greywall, D. S., Yurke, B., Busch, P. A., Pargellis, A. N. & Willett, R. A. Evading amplifier noise in nonlinear oscillators. *Phys. Rev. Lett.* **72,** 2992–2995 (1994).
25. Cleland, A. N. & Roukes, M. L. Fabrication of high frequency nanometer scale resonators from bulk Si crystals. *Appl. Phys. Lett.* **69,** 2653 (1996).
26. Yang, J., Ono, T. & Esashi, M. Surface effects and high quality factors in ultrathin single-crystal silicon cantilevers. *Appl. Phys. Lett.* **77,** 3860–3862 (2000).
27. Yasumura, K. Y. *et al.* Quality factors in micron- and submicron-thick cantilevers. *J. Microelectromech. Syst.* **9,** 117–125 (2000).

Acknowledgements We thank C. Yung, D. Schmidt and S. Aldridge for conversations, and B. Hill for processing support. We acknowledge support provided by the National Science Foundation XYZ-On-A-Chip programme, by the Army Research Office, and by the Office of Naval Research/DARPA SPINS programme.

Competing interests statement The authors declare that they have no competing financial interests.

Correspondence and requests for materials should be addressed to A.N.C. (cleland@physics.ucsb.edu).